Published online 28 February 2012

Nucleic Acids Research, 2012, Vol. 40, No. 11 e82
doi:10.1093/nar/gks203

Comparison of microfluidic digital PCR and conventional quantitative PCR for measuring copy number variation

Alexandra S. Whale[1], Jim F. Huggett[1,*], Simon Cowen[1], Valerie Speirs[2], Jacqui Shaw[3], Stephen Ellison[1], Carole A. Foy[1] and Daniel J. Scott[1]

[1]LGC Limited, Queens Road, Teddington, Middlesex TW11 0LY, [2]Leeds Institute of Molecular Medicine, University of Leeds, St. James's University Hospital, Leeds LS9 7TF and [3]Cancer Studies & Molecular Medicine, University of Leicester, Robert Kilpatrick Clinical Sciences Building, Leicester Royal Infirmary, Leicester LE2 7LX, UK

Received January 5, 2011; Revised and Accepted February 14, 2012

ABSTRACT

One of the benefits of Digital PCR (dPCR) is the potential for unparalleled precision enabling smaller fold change measurements. An example of an assessment that could benefit from such improved precision is the measurement of tumour-associated copy number variation (CNV) in the cell free DNA (cfDNA) fraction of patient blood plasma. To investigate the potential precision of dPCR and compare it with the established technique of quantitative PCR (qPCR), we used breast cancer cell lines to investigate *HER2* gene amplification and modelled a range of different CNVs. We showed that, with equal experimental replication, dPCR could measure a smaller CNV than qPCR. As dPCR precision is directly dependent upon both the number of replicate measurements and the template concentration, we also developed a method to assist the design of dPCR experiments for measuring CNV. Using an existing model (based on Poisson and binomial distributions) to derive an expression for the variance inherent in dPCR, we produced a power calculation to define the experimental size required to reliably detect a given fold change at a given template concentration. This work will facilitate any future translation of dPCR to key diagnostic applications, such as cancer diagnostics and analysis of cfDNA.

INTRODUCTION

A key measurement challenge in diagnostic research involves identifying small changes in gene dosage or nucleic acid sequence that are commonly associated with genetic diseases. Copy number variations (CNVs) are changes in the genomic DNA leading to an abnormal number of copies of a DNA sequence (usually two copies per diploid genome). CNVs are caused by deletions, duplications or structural rearrangements of the genome. CNVs are involved in a large number of complex human diseases such as Down's syndrome (trisomy 21) and many cancers, for example *HER2* gene amplification in breast cancer (BC) (1–5). CNV measurements are used for routine screening in clinical diagnostics and their analysis can assist in subsequent prognostic monitoring (6,7). Clinical diagnostic methods currently include fluorescence *in situ* hybridization (FISH), comparative genome hybridisation (CGH), single nucleotide polymorphism (SNP) arrays, deep sequencing and real-time quantitative PCR (qPCR) (8–10).

Quantitative PCR (qPCR) is currently the most sensitive approach able to resolve ~1.5-fold changes (11,12). The discovery of cell free DNA (cfDNA) in blood plasma has provided a simple source of genetic material for pre-natal and tumour diagnosis (13–18) that could potentially enable routine minimally invasive sampling for subsequent CNV analysis. qPCR has recently identify amplified *HER2* molecules in breast cancer patients with good correlation between the levels of amplification detected in the primary tumour and cfDNA (19). However, as only a proportion of the cfDNA is derived from the embryo or tumour, identification of an associated CNV is more challenging as the target DNA is effectively 'diluted' in a background of normal DNA. Consequently, a tumour-associated 5-fold increase in CNV becomes a 1.2-fold increase if only 5% of the cfDNA sample is derived from the tumour; this magnitude of CNV would be undetectable by current approaches.

One method that has shown promise for improving the limit of detection for nucleic acid quantification is digital PCR (dPCR) with a number of reports highlighting the

*To whom correspondence should be addressed. Tel: +44 20 8943 7655; Fax: +44 20 8943 2767; Email: jim.huggett@lgcgroup.com

superior accuracy of dPCR for CNV analysis (20,21). dPCR has been reported to detect a 1.25-fold difference in copy number (21); however, to our knowledge, no direct comparison between qPCR and dPCR has been performed to ascertain if the latter is more sensitive. Another aspect that is not extensively addressed in the literature is that the ability of dPCR to measure small CNVs is directly dependent upon template concentration. This is a crucial consideration when considering cfDNA as a template as its concentration can range considerably; from 2 to 30 ng/ml plasma in healthy individuals to 180–600 ng/ml plasma both during pregnancy and in cancer patients (13,16,18,22–24).

This study aimed to investigate this further using an *in vitro* BC gene amplification model to identify when a CNV is too small to be measured by qPCR and dPCR. Subsequently, we developed a model, based on the Poisson and binomial distributions, to determine the variance inherent in dPCR, and used this to perform power calculations which demonstrate the effects of the DNA-template concentration on the sensitivity of CNV measurements.

MATERIALS AND METHODS

DNA samples

Genomic DNA (gDNA) from three BC cell lines with different levels of *HER2* gene amplification were used; high-*HER2* amplification (SK-BR-3; ATCC HTB-30), low-level *HER2* gain (T-47D; ATCC HTB-133) and one with a single *HER2* allele deletion (MCF-7; ATCC HTB-22). Control experiments were performed using commercially available gDNA from pooled healthy females that have two copies of each gene per diploid genome (Promega G1521). gDNA concentrations were determined by A_{260} measurements (Nanodrop, Thermo Scientific) and purity was measured by A_{260}/A_{280} measurement (all gDNA samples were between 1.93 and 1.96). Haploid copy number dilutions were calculated based on the molecular weight of one normal haploid female genome equalling 3.275 pg.

Gene-specific assays

The TaqMan® copy number reference assay (Applied Biosystems 4401631) contained 900 nM each of *RNase P*-specific forward and reverse primers and 250 nM of a VIC dye-labelled TAMRA hydrolysis probe. The *RNase P* amplicon sequence was confirmed by clonal sequencing (LGC Genomics; Supplementary Figure S1a). The *HER2* assay, targeting intron 5 of the *HER2* gene on chromosome 17q21.1, contained 900 nM each of forward (5′-AAG CTA AGA AAT AAG GCC AGA TGG-3′) and reverse (5′-CGC ACA GCA CCA AGG AAA AG-3′) primers and 200 nM of hydrolysis probe (5′ FAM-CAG CAG AAC AAC GCA GCC CTC CCT-BHQ1 3′) (20) (SIGMA). The amplification of a single PCR product for both the *RNase P* and *HER2* assays was confirmed using the 2100 Bioanalyzer and DNA 1000 kit according to the manufacturer's instructions (Agilent; Supplementary Figure S1b).

Real-time quantitative PCR

Real-time quantitative PCR was performed in accordance with the MIQE guidelines (Supplementary Table S1 and Supplementary Figure S1) (25). Ten microlitres reactions contained 1× TaqMan® gene expression mastermix (ABI 4369016), 1× gene-specific assay and 2 µl target DNA. qPCR was performed using the Prism 7900HT Real Time PCR system (ABI). Thermocycling conditions were 95°C for 10 min, followed by 40 cycles of 95°C for 15 s and 60°C for 60 s. Quantification was performed with the standard curve method using five standard dilutions, in triplicate, of normal female gDNA ranging from 16.50 to 0.33 ng (5000 to 100 haploid genome copies) per reaction. Due to the differences in molecular weight between the BC cell line gDNA, triplicate reactions were performed on a range of gDNA concentrations (16.50 to 0.33 ng per reaction) for *HER2* and *RNase P* assays. This allowed identification of the gDNA concentration that fell within the range of the qPCR standard curves for both *HER2* and *RNase P* assays. Subsequently, eight *HER2* and eight *RNase P* reactions (16 reactions in total) were performed on the optimum weight of gDNA for each cell line (normal female: 0.71 ng, MCF-7: 0.60 ng, SK-BR-3: 0.94 ng and T-47D: 1.45 ng). The SDS software v2.4 (ABI) was used to calculate the quantification cycle (Cq) value, that is defined as the number of cycles at which the fluorescence signal is significant above the threshold, which was converted to copy number using the relevant standard curve. Replicate *HER2*:*RNase P* ratios were calculated by randomly pairing *HER2* and *RNase P* copy numbers and calculating the 95% confidence intervals (CI) from the standard error of the mean and the two-tailed Student's *t*-test. No template control (NTC) reactions were performed using water with no template; in all cases, no amplification occurred (Supplementary Figure S1c and S1d).

Digital PCR

About 4.5 µl reactions containing 1× TaqMan® gene expression mastermix, 2× GE sample loading reagent (Fluidigm 85000746), 1× gene-specific assay and 1.35 µl target gDNA was pipetted into each loading inlet of a 48.770 digital PCR array (Fluidigm). The BioMark IFC controller MX (Fluidigm, San Francisco, CA) was used to uniformly partition the reaction from the loading inlet into the 770×0.84 nl chambers. dPCR was performed using the BioMark System for Genetic Analysis (Fluidigm). Thermocycling conditions were set as for qPCR. For BC cell line gDNA analysis, reactions were performed in quadruplicate panels for *HER2* and *RNase P* assays (eight panels in total) on 0.6 ng BC cell line gDNA, estimated using A_{260} measurements. The Digital PCR Analysis software (Fluidigm) was used to set the Cq threshold and range (Supplementary Figure S2), and to count the number of positive chambers (H) out of the total number chambers (C) from which the Poisson distribution was used to estimate the average number of molecules per chamber (λ) so that $\lambda = -\ln(1 - H/C)$ (26). *HER2*:*RNase P* ratio (λ_t/λ_r) and 95% CI were calculated as described in this publication (Table 1). NTC reactions were performed using water with no template; in all cases,

Table 1. Summary of equations derived in this study

Description	Symbol	Equation	Equation in MS Excel	Worked example
Number of chambers analysed	C			770
Number of positive chambers for reference	H_r			140
Number of positive chambers for target	H_t			180
Number of reference molecules per chamber	λ_r	$-\ln(1 - H_r/C)$	$-\ln(1 - (H_r/C))$	0.201
Number of target molecules per chamber	λ_t	$-\ln(1 - H_t/C)$	$-\ln(1 - (H_t/C))$	0.266
Log ratio estimate	R	$\ln(\lambda_t/\lambda_r)$	$\ln(\lambda_t/\lambda_r)$	0.283
Variance for Log ratio estimate	${\sigma_R}^2$	$\frac{1-e^{-\lambda_t}}{C\lambda_t^2 e^{-\lambda_t}}+\frac{1-e^{-\lambda_r}}{C\lambda_r^2 e^{-\lambda_r}}$	(1 − EXP(−λ_t))/($C \times {\lambda_t}^2$ * EXP(−λ_t)) +(1 − EXP(−λ_r))/(C * λ_r2 * EXP(−λ_r))	0.002
Standard deviation for Log ratio estimate	σ_R	$\sqrt{\frac{1-e^{-\lambda_t}}{C\lambda_t^2 e^{-\lambda_t}}+\frac{1-e^{-\lambda_r}}{C\lambda_r^2 e^{-\lambda_r}}}$	SQRT($\sigma_R{}^2$)	0.040
Log ratio 95% CI (one-tailed) - high	RCI-H	$R+1.960\sigma_R$	R+NORMSINV(0.975) * σ_R	0.361
Log ratio 95% CI (one-tailed) - low	RCI-L	$R-1.960\sigma_R$	R+NORMSINV(0.025) * σ_R	0.205
Ratio	R	e^R	EXP(R)	1.327
Ratio 95% CI (one-tailed) - high	RCI-H	$e^{R\text{CI-H}}$	EXP(RCI-H)	1.435
Ratio 95% CI (one tailed) - low	RCI-L	$e^{R\text{CI-L}}$	EXP(RCI-L)	1.227

For equations in MS Excel, an 'equals' sign must be inserted before the formula and symbols should be replaced with the experimental values. A worked example is provided, with the values used to generate the variance model and to ensure correct equations are transferred

no positive chambers were observed (Supplementary Figure S2).

Establishment and analysis of copy number variation ratios

The *in vitro* gene amplification model was established by spiking T-47D gDNA into normal female gDNA at various percentages to generate a theoretical range of *HER2*:*RNase P* ratios between 1.00 and 2.00 based on the dPCR analysis (Supplementary Table S2). All ratios were diluted to give approximately 720 *RNase P* copies/µl. For qPCR, four replicates were performed per ratio for both *HER2* and *RNase P* assays in two independent experiments (16 reactions in total). All CNV ratios were calculated by conversion of Cq values to copy numbers of *HER2* and *RNase P* using a standard curve generated from five dilutions, in triplicate, of normal female gDNA ranging from 1,000 to 20 haploid genome copies/µl (Supplementary Figure S1c and S1d). For dPCR, four panels were performed per ratio for both *HER2* and *RNase P* assays in two independent experiments (16 panels in total) to give approximately 155 *RNase P* copies per panel ($\lambda_r = 0.2$) where one panel on a 48.770 dPCR array contains 0.195 µl of template. CNV ratios were calculated using the equations described in this paper (Table 1).

To investigate the number of dPCR panels (containing 770 chambers each) needed to detect small ratio differences, a pseudo-random number generator (the 'Math.random()' method in JavaScript) was used to assign a number to each *HER2* and *RNase P* panel. In each case, the required numbers of panels were selected from the eight panel data set.

Statistical analysis and power calculations

Statistical analysis was performed using the MS Office Excel software (2003). Statistical comparisons to establish CNV limit of measurement were performed using the one-way analysis of variance test to compare the *RNase P* counts (dPCR) or copy number (qPCR) between the samples (*in vitro* gene amplification model ratio). Two-way analysis of variance was used to test for differences in the mean copy number between the respective replicate qPCR experiments. The two-tailed Student's *t*-test was used to analyse the difference in *HER2* counts or copy number between the sample and the calibrator (normal female gDNA). Power and associated calculations reported in this paper were carried out using the R statistical programming language (version 2.13, http://www.r-project.org). All scripts were written and run on a standard desktop personal computer (Optiplex, Dell Corporation). Further details of the methods and theory are given in the Statistical Supplementary Information.

RESULTS

CNV measurement by dPCR and comparison with qPCR

In order to investigate the accuracy of dPCR for CNV measurement, we used three BC cell lines with different *HER2* gene copy number as a model of gene amplification. The *RNase P* assay was used as the reference gene for the diploid control. Assay optimization was performed using qPCR for *HER2* and *RNase P* assays (Supplementary Figure S1). For dPCR, absolute quantification of *HER2* and *RNase P* molecules were calculated from the number of positive counts per panel based on the Poisson distribution for the number of molecules in each chamber (Figure 1a).

dPCR analysis of normal female gDNA had a *HER2:RNase P* ratio of 1.03 and was not significantly different from qPCR analysis that had a *HER2*:*RNase P* ratio of 1.00 ($P = 0.39$; Figure 1b). Analysis of MCF-7 gDNA, which has a single *HER2* allele deletion, gave a ratio of 0.44 by both dPCR and qPCR. T-47D gDNA, which has low-*HER2* copy gain had a *HER2*:*RNase P* ratio of 2.00 and 1.96 for dPCR and qPCR, respectively. There was no significant difference in *HER2*:*RNase P* ratios between the two techniques when measuring

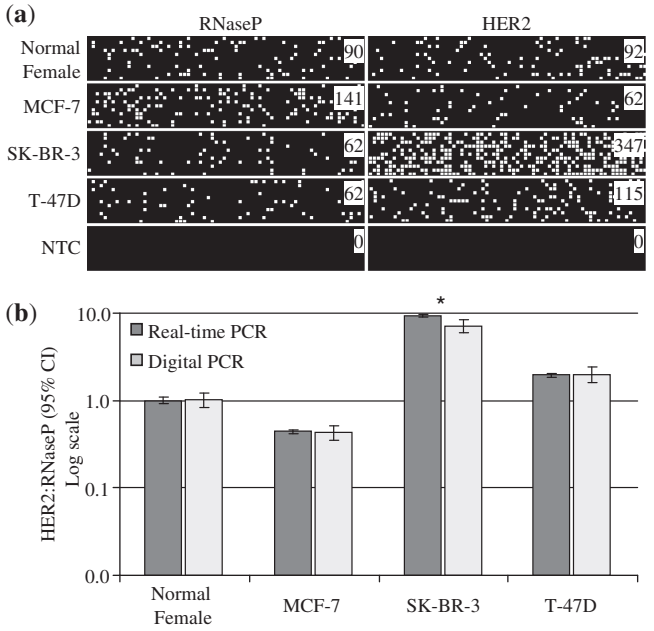

Figure 1. Comparison of *HER2:RNase P* ratio in breast cancer cell line genomic DNA using digital and quantitative real-time PCR. (**a**) Software-generated heat map showing a single panel in a 48.770 dPCR array that contains 770 chambers with positive (white) and negative (black) amplification signals. One representative dPCR panel is shown for each gDNA sample and assay with the number of positive chambers shown in the top right corner of the panel. Positive and negative chambers were used to calculate the number of molecules per panel and the *HER2:RNase P* ratio for the gDNA sample. The NTC panels for both assays had no positive chambers. (**b**) qPCR ($n = 8$ wells) and dPCR ($n = 4$ panels) gave similar *HER2:RNase P* ratios for all BC gDNA except the SK-BR-3 gDNA that was significantly higher by qPCR compared with dPCR (asterisk). Data is presented on a log scale and error bars represent 95% CIs.

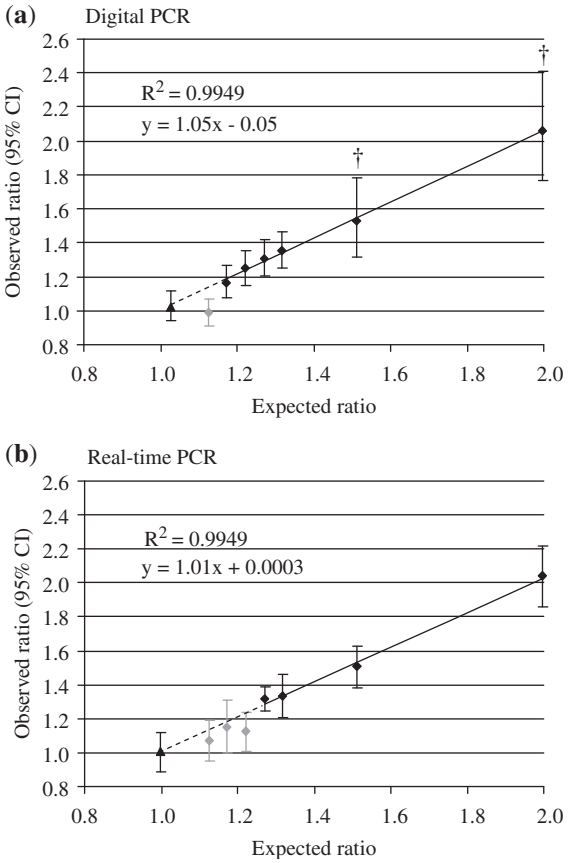

Figure 2. Determination of CNV detection of digital and quantitative real-time PCR. Quantitation of *HER2:RNase P* ratios using (**a**) dPCR and (**b**) qPCR generated from the *in vitro* gene-amplification model. The *x*-axis shows the expected *HER2:RNase P* ratio and the *y*-axis shows the observed *HER2:RNase P* ratios with the 95% CI. (a) For dPCR, four panels for each assay were analyzed for ratios > 1.5 (daggered symbol) and eight panels for each assay for ratios <1.5. In all cases, λ_r was approximately 0.2. The error bars represent the 95% CIs. (b) For qPCR, eight reactions were performed for each assay and all ratios. The error bars represent the 95% CIs calculated from the standard error of the mean and associated *T*-value with 95% confidence and seven degrees-of-freedom. Key: *black triangle*: normal female gDNA, *black diamond*: significantly different from normal female gDNA ($P < 0.05$), *gray diamond*: not significantly different from normal female gDNA ($P > 0.05$). *Solid line* of linear correlation is shown for those ratios that were significantly different from normal female gDNA. *Dashed line* is the extrapolation of the linear correlation showing intersection with *HER2:RNase P* ratio of 1.0. R^2 and equations are given for the linear correlation.

MCF-7 ($P = 0.71$) and T-47D ($P = 0.52$). SK-BR-3 gDNA, which has high *HER2* gene amplification, had a *HER2*:*RNase P* ratio of 7.15 when measured by dPCR which was significantly lower than the *HER2*:*RNase P* ratio 9.43 observed by qPCR ($P = 0.00005$). For all measurements, the 95% CIs were slightly larger for dPCR, where four dPCR panels were analyzed, when compared with qPCR, where eight reaction wells were analyzed (Figure 1b).

Limit of detection for analysing copy number variations

To determine the limit of detection for analysis of CNVs by dPCR, an *in vitro* gene-amplification model was used, whereby T-47D gDNA was spiked into normal female gDNA to generate a theoretical range of *HER2*:*RNase P* ratios between 1.00 and 2.00 at low copy number (2.1 ng/μl) for analysis using dPCR and qPCR (Supplementary Table S2). Using dPCR, a ratio of 1.17 or more was significantly different from the experimentally derived normal female gDNA ratio of 1.03 ($P < 0.0003$) when eight panels where used (Figure 2a). There was good linear correlation between the expected and the observed ratios when measuring a CNV of ≥1.17 ($R^2 = 0.9974$) and this linear correlation was maintained when the line was extrapolated through the observed ratio for normal female gDNA (Figure 2a; dashed line). Furthermore, the slope and intercept of the linear correlation were measured as 1.05 and 0.05, respectively, demonstrating the accuracy in the measured ratios, and that no bias was introduced. An expected ratio of 1.12 was not significantly different from normal female gDNA when using eight panels ($P = 0.67$; Figure 2a). In all cases, the *RNase P* counts observed for each measurement were not significantly different from one another ($P \geq 0.75$). Analysing the *in vitro* gene-amplification model with qPCR demonstrated that ratios of 1.27 or more were significantly different from

normal female gDNA ($P < 0.0005$) and maintained a linear correlation ($R^2 = \geq 0.99$; Figure 2b; dashed line). As was observed with the dPCR analysis, the observed ratios were accurate with no introduced bias as shown by the slope (1.01) and intercept (<0.001) of the linear correlation. Ratios of ≤1.22 did not differ significantly from female gDNA ($P > 0.05$; Figure 2b). As with dPCR, in all cases, the *RNase P* counts observed for each measurement were not significantly different from one another ($P \geq 0.27$). Furthermore, no statistically significant inter-run variability was observed for either the *RNase P* or the *HER2* assays ($P \geq 0.99$ and $P \geq 0.15$, respectively).

Determination of the number of dPCR panels needed to confidently detect small changes in copy number variation

From our data, when the CNV to be measured is >1.5-fold, then four dPCR panels were sufficient while CNVs < 1.5-fold could be detected with up to eight dPCR panels (Figures 1b and 2a). As CNVs of <1.17 were not measurable using eight dPCR panels, it would be useful to be able to predict how many dPCR panels would be needed to detect such small CNVs. For such a prediction, we would need to assess discriminating power, and therefore, the true copy number difference at which we would reliably judge two materials to be different. This was achieved with a statistical power calculation, which required a test statistic and associated distribution.

The domain of interest in this study involved the reference *RNase P* assay adjusted to give an observed number of positive chambers in the region of 100–200 per panel (2.1 ng/μl) to mimic the low concentration observed in cfDNA samples (18). Based on the Poisson distribution, this can be used to estimate the number of molecules per chamber (λ), and in this case, λ was approximately 0.2 in a 48.770 dPCR array (Table 1). At this concentration, the probability P that a chamber will give a positive signal is $1 - e^{-\lambda}$ and is the same for every chamber (26). The CNV is the ratio of λ estimates for the two groups being compared and as such, it is highly non-Normal. By taking the logarithm of the ratio for these two groups (R), the data is transformed to produce a variable whose distribution is very close to Normal (Supplementary Figure S3a) and is given by the equation:

$$R = \ln \frac{\lambda_t}{\lambda_r} \quad (1)$$

where λ_t and λ_r correspond to the λ values of the target and reference genes, respectively, and $\lambda = -\ln(1 - H/C)$ [Table 1; (26)]. Consequently, power calculations can be based on a *t*-test for a difference in the logarithm of the observed ratio of target to reference gene from zero. To calculate power, we first need an expression for the variance (σ_R^2) of the log ratio R. This was derived using first-order error propagation (see 'Statistical Supplementary Information') and is given here as:

$$\sigma_R^2 \approx \frac{1 - e^{-\lambda_t}}{C\lambda_t^2 e^{-\lambda_t}} + \frac{1 - e^{-\lambda_r}}{C\lambda_r^2 e^{-\lambda_r}} \quad (2)$$

Comparison of the theoretical standard deviation of R [estimated from Equation (2) as $\sqrt{\sigma_R^2}$] with the observed standard deviation of the experimental data (Figure 2a) demonstrated good concordance (Supplementary Figure S3b). With a valid estimate of the variance σ_R^2 in the log ratio, the upper and lower 95% CI can be calculated (Table 1). Power calculations can also be derived to determine the number of chambers required for an experiment capable of detecting a log ratio R with a defined test power of $1 - \beta$ and at the $1 - \alpha$ confidence level, where α and β are the false-positive and false-negative rates, respectively. Our experiment was one in which a positive R was the expected result (an increase in copy number, so $\lambda_t > \lambda_r$), so a one-tailed test was appropriate. Statistical significance was declared at a P-value of α or lower (<0.05) and the test power was equal to 95% (where $\beta = 0.05$; Supplementary Figure S4). Power calculations involving a test statistic which has a Normal distribution can only be carried out numerically, as there is no analytical solution and details of the method are given in the 'Statistical Supplementary Information'.

Using the power curve, where $\lambda_r = 0.2$, we found that with 95% power, a fold change of 1.2 was easily detectable with five 770-chamber panels per gene assay, while ratios of 1.1 and below required greatly increased numbers of panels (>15 panels; Figure 3a). Using the curve to compare the data from the *HER2 in vitro* gene-amplification model with the number of panels required demonstrates that a ≥1.17 ratio can be measured with eight or fewer panels (Figure 3a); this is shown experimentally (Figure 2a). However, from the curve, a ratio of 1.12 was predicted to need more than 10 panels (Figure 3a), which is supported by our inability to measure with confidence a 1.12 ratio with only eight panels (Figure 2a). Our power curve predicts that when λ_r is 0.2, the smallest CNV ratio that could be measured using eight dPCR panels is approximately 1.15 (Figure 3a). This lies between our two experimental data points and therefore confirms the fitness of our model for this template concentration.

To further test the power calculations, each *HER2* dPCR panel was randomly paired with an *RNase P* panel and the desired number of paired panels (1–8) were selected and used to calculate their CNV ratio and associated 95% CI (Figure 3b). Our power curve suggests that approximately three panels are needed to detect a ratio of 1.27 when $\lambda_r = 0.2$ (Figure 3a) which was experimentally measurable with four or more panels (Figure 3b). Analysis of a fold difference of 1.17 predicted that approximately six panels are needed (Figure 3a), which is concordant with our experimental data (Figure 3b).

Power calculations were also performed for qPCR using the Student's *t*-statistic (see 'Supplementary Statistical Information' for details) and the resulting power curves demonstrated that ratios greater than 1.25 can be measured with 95% power and eight replicate qPCR wells (Supplementary Figure S7). This compared well with the experimental data generated from the *in vitro* gene amplification model where a ratio of 1.27 was measured with eight qPCR wells but small ratios were not (Figure 2b). From the power curve, it was shown that using gDNA at the experimental defined

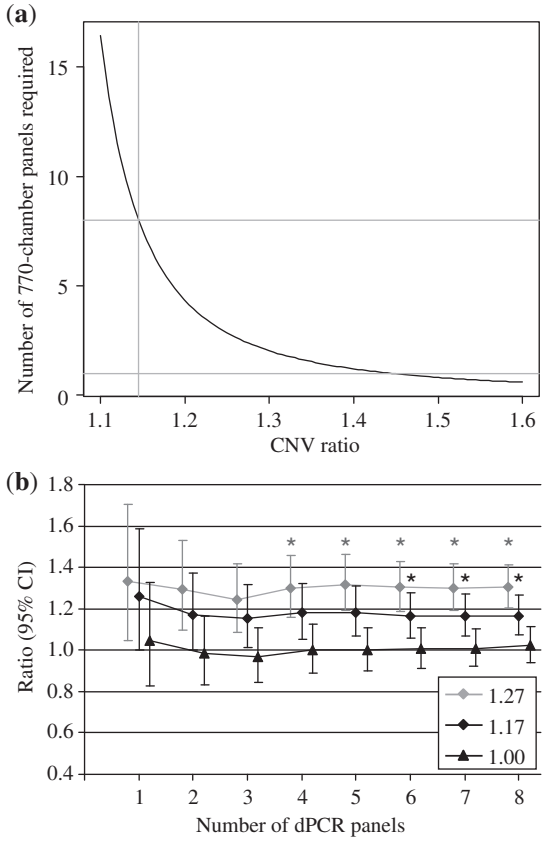

Figure 3. Determination of the number of dPCR panels needed to measure *HER2:RNase P* ratios. (**a**) Power curve to determine the number of panels required to detect different ratios of λ_t to λ_r, where $\lambda_t > \lambda_r$ with 95% power at a confidence level of 95% and $\lambda_r = 0.2$. The two horizontal lines show a single-panel and eight-panel experiment where the intersections with the power curve indicates the lowest detectable CNV. The vertical line shows the smallest CNV detectable is approximately 1.15 when $\lambda_r = 0.2$ and the number of panels is 8. (**b**) The relevant number of dPCR panels (1–8) were selected and the *HER2:RNase P* ratio and associated 95% CIs were calculated. The graphs for the different ratios are slightly staggered to allow identification of the 95% CI error bars for each ratio. Ratios that are statistically different from the normal female gDNA are shown for ratios of 1.27 (gray asterisk) and 1.17 (black asterisk).

concentration, an excess of 20 qPCR wells would be needed to measure ratios of 1.17 or fewer (Supplementary Figure S7).

DISCUSSION

We have investigated the measurement capabilities of dPCR when investigating changes in CNV, described the limit of detection for a given experiment and demonstrate that dPCR exhibits greater sensitivity than qPCR when investigating subtle fold-differences. The potential of cfDNA as a source of template in minimally invasive diagnostics is becoming increasingly apparent. The measurable resolution of qPCR in our gene-amplification model for cfDNA, which we describe here as a ratio of 1.27, offers a theoretical diagnostic potential, however, the reality is that smaller CNVs, where the tumour contribution to the cfDNA can be as little as 5% of the total cfDNA (16,17) are still technically out of reach using qPCR. Furthermore, one of the major differences between qPCR and dPCR is that technical variability of qPCR can be high between and within laboratories (27). dPCR is notably less variable between experiments (28,29), which offers the possibility of reproducibly more accurate results. In this study, a CNV ratio of 1.17 was significantly detected using eight panels and therefore, the ability of dPCR to detect incrementally smaller fold differences than qPCR demonstrates the potential of this method for future CNV clinical diagnostics.

Recently, an error model relating to the 95% theoretical CI for copy number versus number of chambers was published (21). According to this model, approximately 1,200 chambers (equates to 1.5 panels) would be needed to detect a CNV ratio of 1.25. However, when the authors performed this in a real experiment, they were unable to realise this predicted precision, requiring twice the number of chambers/panels to measure the targeted difference (21). The authors explain that this was directly due to the fact that, for their model, they fixed the λ_r at a value of 0.6, whereas the real experiment (where λ_r values were 0.18 and 0.37 for their two samples) was below this value and so did not have sufficient power to resolve the given difference with the predicted number of chambers.

When we used this model to estimate the number of chambers needed for our experiments, we found that this was also underestimated and due to the smaller λ_r, which in the case of our experiment was about 0.2. Weaver and co-workers (21) used the point (in observed number of panels) at which calculated 95% CIs just overlap, assuming a Poisson distribution for individual counts. The point of theoretical CI overlap is an indicator of discriminating power, in that it increases as precision degrades and allows comparison between samples. However, basic statistical theory shows that a significant difference at the 95% confidence level would usually show substantially overlapping CIs for the two independent observations. In this case, statistical significance focuses on the error rate under the null hypothesis; the probability of wrongly declaring a result significant, or the false-positive rate. In contrast, we were interested in assessing discriminating power and therefore, the true copy number difference at which will we reliably judge two materials to be different, that is the false-negative rate. Therefore, we generated a power calculation based on the variance and false-negative rate of a given measurement of copy number ratio.

Our power calculation method takes the DNA-template concentration into consideration using the corresponding λ_r and estimating the number of panels required. Validation of the theory is demonstrated with our experimental data (Figure 3b). Based on this, further theoretical power curves for a range of λ_r values (0.1–0.8) were derived and are given in Supplementary Figure S5 for researchers to use for future experimental design. From these power curves, we predict that to investigate a 1.25-fold difference, where λ_r is 0.2 or 0.4 (approximate values for λ_r of 0.18 and 0.37) with 95% power requires a four- or two-panel experiment,

respectively (Supplementary Figure S5), which was consistent with Weaver and co-workers observations. The power calculations described in this publication are based on a one-tailed test as we were interested detecting *HER2* amplification (where $\lambda_t > \lambda_r$) which has clinical and prognostic relevance (30,31). Further applications of this model would include detection of trisomy, e.g. in Down's syndrome (32). However, a modification of this model to include detection of both amplification and deletion of gene copies would have a wider scope, e.g. in characterization of *in vitro* culture cells over time (33), detection of polyploidy in plants (34) or as an alternative to CGH analysis or FISH for cancer diagnostics. Therefore, we have expanded our model to incorporate a two-tail test (Supplementary Figure S6).

We also generated power curves for qPCR based on a one- or two-tailed test (Supplementary Figure S7). These curves demonstrates that while dPCR appears to detect only incrementally smaller fold differences than qPCR using a one-tailed test and eight replicate measurements (1.17 versus 1.27 in this study), an additional 12 qPCR wells per assay or more would be needed before qPCR could potentially measure a similarly small ratio to dPCR. This is dependent upon the standard deviation of the qPCR (in this case, was approximately 10% for both assays across all experiments) as the number of replicates needed will increase if precision is reduced. The binary nature of dPCR means that the precision is more independent of variation in assay amplification, making it easier to optimize and standardize between laboratories.

As conventional qPCR is currently approximately one 20th of the expense of an equivalent dPCR analysis, it does still offer a practical alternative method to measure smaller CNVs. However, the increased template required to perform the larger number of replicate measurements could be a disadvantage where sample is limiting. qPCR has the benefit of being able to measure lower plasma template concentration than the dPCR method used here as its larger reaction volume facilitates the addition of more template. qPCR is also scalable offering the option of adding even more template, where sample permits, by further increasing the volume of the reaction. This is not currently possible with the dPCR approach used here; however, with the development of higher volume and throughput dPCR methods this option will also be possible (35–37) with comparable accuracy (38).

Improvements to qPCR using similar technologies to those advancing dPCR will increase the throughput of qPCR, as has already been described (21), although this is also at the cost of smaller input volume which often requires pre-amplification (39); this is not routinely needed for dPCR. It should also be noted that for qPCR (conventional or high throughput) to measure such small fold changes, it is not only important that precise well-optimized assays are used, but it is also essential that some estimation of efficiency is made (25). This can be done by standard curves to estimate copy number, as described here, or by performing efficiency corrected $\Delta\Delta$Cq (40). However, this fact further complicates using qPCR for small fold change measurement.

Our model also raises the question of why variable λ_r should need to be considered at all when performing dPCR. The alternative would be to ensure the optimum concentration in the first place. However, this is only possible when the sample DNA is at or higher than this value, and if the concentration is lower than the optimum λ_r then more chambers would be needed, and therefore, our model would provide an idea of how many. This issue is applicable when using cfDNA as a template, which is by nature low in concentration; around 2–30 ng/ml blood plasma in normal healthy humans (13,16–18,22,23), which corresponds to approximately 600–9900 normal haploid genomes per ml. Measuring *HER2* status using cfDNA offers considerable potential as a diagnostic and prognostic test (19,30,31).

Our power calculation provides a good foundation from which to design subsequent experiments; in our assessment, we have used a high-quality DNA template in our proof-of-principle experiments to model the cfDNA. Additional factors that will need to be considered, building on the findings of this study, include template integrity, PCR-assay efficiency and the impact of matrix effects as integral parts of subsequent translational research, if this approach is to be used in the context of *HER2* and other clinical measurements. Recently, power calculations based on a multivolume dPCR assays were generated and demonstrated that different reaction volumes influence the dynamic range and precision of dPCR, could minimize the total number of dPCR reactions needed and separated the upper and lower limits of quantification. This would allow samples of differing concentration to be analyzed in parallel without compromising one sample over the other (37).

An additional function of this study was to directly compare microfluidic dPCR with conventional qPCR for CNV using the same gDNA template and reaction assays. Both methods gave similar *HER2* CNV results using BC cell line gDNA with varying numbers of *HER2* gene copies per diploid genome. Two BC cell lines were concurrent with the published data; MCF-7 gDNA, that has monosomy for chromosome 17 assigned a *HER2:RNase P* ratio of < 0.5 (one copy per diploid genome) (41,42) and T-47D gDNA gave a *HER2:RNase P* ratio of < 2 (3–4 copies per diploid genome) (43–46). Analysis of the SK-BR-3 gDNA identified high levels of *HER2* amplification that corresponds with the published copy number range (14–24 copies per diploid genome) (41,43–45,47). However, there was a discrepancy between the *HER2:RNase P* ratio obtained by dPCR (7.15) and qPCR (9.43).

This difference could be attributed to the large number of *HER2* gene amplifications occurring on the same molecule (concatamers of *HER2* molecules inserted at the same point in the genome) that are observed in this cell line using FISH (48,49) but do not occur in the MCF-7 or T-47D cell lines. Unlike qPCR, dPCR may be unable to accurately quantify this type of gene amplification as linked genes cannot be separated into individual chambers. Qin and co-workers (20) have suggested that this problem can be overcome by a pre-amplification step using gene-specific primers to separate the linked

copies before performing dPCR. However, such a step requires careful validation because of the potential bias that can be introduced that may outweigh the necessary precision for detecting small CNVs (29).

In conclusion, our data suggests as microfluidic dPCR becomes more established, it will offer a new level of precision and the clinical benefits of measuring smaller CNVs in more challenging samples like cfDNA, will become possible. However, the pre-clinical and translational research necessary for this to be realized will need to consider the issues explored by this study. The model we describe here both provides a mechanism to facilitate this research and highlights the issues around ensuring the template concentration is included as a central consideration when preparing CNV studies using dPCR. This will better enable dPCR experiments to be designed, increasing the impact of future research.

SUPPLEMENTARY DATA

Supplementary Data are available at NAR Online: Supplementary Tables 1–2, Supplementary Figures 1–7 and Supplementary Statistical Information.

ACKNOWLEDGEMENTS

The authors would like to acknowledge Dr Malcolm Burns and Dr Alison Devonshire for critical review of the manuscript.

FUNDING

The UK National Measurement System. Funding for open access charge: UK National Measurement System (UK Government).

Conflict of interest statement. None declared.

REFERENCES

1. Shlien,A. and Malkin,D. (2010) Copy number variations and cancer susceptibility. *Curr. Opin. Oncol.*, **22**, 55–63.
2. Wain,L.V., Armour,J.A. and Tobin,M.D. (2009) Genomic copy number variation, human health, and disease. *Lancet*, **374**, 340–350.
3. McCarroll,S.A. and Altshuler,D.M. (2007) Copy-number variation and association studies of human disease. *Nat. Genet.*, **39**, S37–S42.
4. Reese,D.M. and Slamon,D.J. (1997) HER-2/neu signal transduction in human breast and ovarian cancer. *Stem Cells*, **15**, 1–8.
5. Slamon,D.J., Clark,G.M., Wong,S.G., Levin,W.J., Ullrich,A. and McGuire,W.L. (1987) Human breast cancer: correlation of relapse and survival with amplification of the HER-2/neu oncogene. *Science*, **235**, 177–182.
6. Shlien,A. and Malkin,D. (2009) Copy number variations and cancer. *Genome Med.*, **1**, 62.
7. Ionita-Laza,I., Rogers,A.J., Lange,C., Raby,B.A. and Lee,C. (2009) Genetic association analysis of copy-number variation (CNV) in human disease pathogenesis. *Genomics*, **93**, 22–26.
8. Lee,C., Iafrate,A.J. and Brothman,A.R. (2007) Copy number variations and clinical cytogenetic diagnosis of constitutional disorders. *Nat. Genet.*, **39**, S48–S54.
9. Xie,C. and Tammi,M.T. (2009) CNV-seq, a new method to detect copy number variation using high-throughput sequencing. *BMC Bioinform.*, **10**, 80.
10. Zhang,F., Gu,W., Hurles,M.E. and Lupski,J.R. (2009) Copy number variation in human health, disease, and evolution. *Annu. Rev. Genom. Hum. Genet.*, **10**, 451–481.
11. Chiu,R.W., Murphy,M.F., Fidler,C., Zee,B.C., Wainscoat,J.S. and Lo,Y.M. (2001) Determination of RhD zygosity: comparison of a double amplification refractory mutation system approach and a multiplex real-time quantitative PCR approach. *Clin. Chem.*, **47**, 667–672.
12. Zimmermann,B., Holzgreve,W., Wenzel,F. and Hahn,S. (2002) Novel real-time quantitative PCR test for trisomy 21. *Clin. Chem.*, **48**, 362–363.
13. Leon,S.A., Shapiro,B., Sklaroff,D.M. and Yaros,M.J. (1977) Free DNA in the serum of cancer patients and the effect of therapy. *Cancer Res.*, **37**, 646–650.
14. Stroun,M., Anker,P., Lyautey,J., Lederrey,C. and Maurice,P.A. (1987) Isolation and characterization of DNA from the plasma of cancer patients. *Eur. J. Cancer Clin. Oncol.*, **23**, 707–712.
15. Hahn,S., Jackson,L.G., Kolla,V., Mahyuddin,A.P. and Choolani,M. (2009) Noninvasive prenatal diagnosis of fetal aneuploidies and Mendelian disorders: new innovative strategies. *Expert Rev. Mol. Diagn.*, **9**, 613–621.
16. Levenson,V.V. (2007) Biomarkers for early detection of breast cancer: what, when, and where? *Biochim. Biophys. Acta*, **1770**, 847–856.
17. Fleischhacker,M. and Schmidt,B. (2007) Circulating nucleic acids (CNAs) and cancer: a survey. *Biochim. Biophys. Acta*, **1775**, 181–232.
18. Jung,K., Fleischhacker,M. and Rabien,A. (2010) Cell-free DNA in the blood as a solid tumor biomarker–a critical appraisal of the literature. *Clin. Chim. Acta*, **411**, 1611–1624.
19. Page,K., Hava,N., Ward,B., Brown,J., Guttery,D.S., Ruangpratheep,C., Blighe,K., Sharma,A., Walker,R.A., Coombes,R.C. *et al.* (2011) Detection of HER2 amplification in circulating free DNA in patients with breast cancer. *Br. J. Cancer*, **104**, 1342–1348.
20. Qin,J., Jones,R.C. and Ramakrishnan,R. (2008) Studying copy number variations using a nanofluidic platform. *Nucleic Acids Res.*, **36**, e116.
21. Weaver,S., Dube,S., Mir,A., Qin,J., Sun,G., Ramakrishnan,R., Jones,R.C. and Livak,K.J. (2010) Taking qPCR to a higher level: analysis of CNV reveals the power of high throughput qPCR to enhance quantitative resolution. *Methods*, **50**, 271–276.
22. Fournie,G.J., Gayral-Taminh,M., Bouche,J.P. and Conte,J.J. (1986) Recovery of nanogram quantities of DNA from plasma and quantitative measurement using labeling by nick translation. *Anal. Biochem.*, **158**, 250–256.
23. Giacona,M.B., Ruben,G.C., Iczkowski,K.A., Roos,T.B., Porter,D.M. and Sorenson,G.D. (1998) Cell-free DNA in human blood plasma: length measurements in patients with pancreatic cancer and healthy controls. *Pancreas*, **17**, 89–97.
24. Diehl,F., Li,M., Dressman,D., He,Y., Shen,D., Szabo,S., Diaz,L.A. Jr, Goodman,S.N., David,K.A., Juhl,H. *et al.* (2005) Detection and quantification of mutations in the plasma of patients with colorectal tumors. *Proc. Natl Acad. Sci. USA*, **102**, 16368–16373.
25. Bustin,S.A., Benes,V., Garson,J.A., Hellemans,J., Huggett,J., Kubista,M., Mueller,R., Nolan,T., Pfaffl,M.W., Shipley,G.L. *et al.* (2009) The MIQE guidelines: minimum information for publication of quantitative real-time PCR experiments. *Clin. Chem.*, **55**, 611–622.
26. Dube,S., Qin,J. and Ramakrishnan,R. (2008) Mathematical analysis of copy number variation in a DNA sample using digital PCR on a nanofluidic device. *PLoS One*, **3**, e2876.
27. Fryer,J.F., Baylis,S.A., Gottlieb,A.L., Ferguson,M., Vincini,G.A., Bevan,V.M., Carman,W.F. and Minor,P.D. (2008) Development of working reference materials for clinical virology. *J. Clin. Virol.*, **43**, 367–371.
28. Bhat,S., Herrmann,J., Armishaw,P., Corbisier,P. and Emslie,K.R. (2009) Single molecule detection in nanofluidic digital array enables accurate measurement of DNA copy number. *Anal. Bioanal. Chem.*, **394**, 457–467.

29. Sanders,R., Huggett,J.F., Bushell,C.A., Cowen,S., Scott,D.J. and Foy,C.A. (2011) Evaluation of digital PCR for absolute DNA quantification. *Anal. Chem.*, **83**, 6474–6484.
30. Dinh,P., de Azambuja,E., Cardoso,F. and Piccart-Gebhart,M.J. (2008) Facts and controversies in the use of trastuzumab in the adjuvant setting. *Nat. Clin. Pract. Oncol.*, **5**, 645–654.
31. Slamon,D.J., Leyland-Jones,B., Shak,S., Fuchs,H., Paton,V., Bajamonde,A., Fleming,T., Eiermann,W., Wolter,J., Pegram,M. *et al.* (2001) Use of chemotherapy plus a monoclonal antibody against HER2 for metastatic breast cancer that overexpresses HER2. *N. Engl. J. Med.*, **344**, 783–792.
32. Fan,H.C. and Quake,S.R. (2007) Detection of aneuploidy with digital polymerase chain reaction. *Anal. Chem.*, **79**, 7576–7579.
33. Hughes,P., Marshall,D., Reid,Y., Parkes,H. and Gelber,C. (2007) The costs of using unauthenticated, over-passaged cell lines: how much more data do we need? *Biotechniques*, **43**, 575–584.
34. Fitzgerald,T.L., Kazan,K., Li,Z., Morell,M.K. and Manners,J.M. (2010) A high-throughput method for the detection of homologous gene deletions in hexaploid wheat. *BMC Plant. Biol.*, **10**, 264.
35. Hatch,A.C., Fisher,J.S., Tovar,A.R., Hsieh,A.T., Lin,R., Pentoney,S.L., Yang,D.L. and Lee,A.P. (2011) 1-Million droplet array with wide-field fluorescence imaging for digital PCR. *Lab Chip*, **11**, 3838–3845.
36. Hindson,B.J., Ness,K.D., Masquelier,D.A., Belgrader,P., Heredia,N.J., Makarewicz,A.J., Bright,I.J., Lucero,M.Y., Hiddessen,A.L., Legler,T.C. *et al.* (2011) High-throughput droplet digital PCR system for absolute quantitation of DNA copy number. *Anal. Chem.*, **83**, 8604–8610.
37. Kreutz,J.E., Munson,T., Huynh,T., Shen,F., Du,W. and Ismagilov,R.F. (2011) Theoretical design and analysis of multivolume digital assays with wide dynamic range validated experimentally with microfluidic digital PCR. *Anal. Chem.*, **83**, 8158–8168.
38. Pinheiro,L.B., Coleman,V.A., Hindson,C.M., Herrmann,J., Hindson,B.J., Bhat,S. and Emslie,K.R. (2012) Evaluation of a droplet digital polymerase chain reaction format for DNA copy number quantification. *Anal. Chem.*, **84**, 1003–1011.
39. Devonshire,A.S., Elaswarapu,R. and Foy,C.A. (2011) Applicability of RNA standards for evaluating RT-qPCR assays and platforms. *BMC Genom.*, **12**, 118.
40. Pfaffl,M.W. (2001) A new mathematical model for relative quantification in real-time RT-PCR. *Nucleic Acids Res.*, **29**, e45.
41. Konigshoff,M., Wilhelm,J., Bohle,R.M., Pingoud,A. and Hahn,M. (2003) HER-2/neu gene copy number quantified by real-time PCR: comparison of gene amplification, heterozygosity, and immunohistochemical status in breast cancer tissue. *Clin. Chem.*, **49**, 219–229.
42. Winnard,P. Jr, Glackin,C. and Raman,V. (2006) Stable integration of an empty vector in MCF-7 cells greatly alters the karyotype. *Cancer Genet. Cytogenet.*, **164**, 174–176.
43. Sestini,R., Orlando,C., Zentilin,L., Lami,D., Gelmini,S., Pinzani,P., Giacca,M. and Pazzagli,M. (1995) Gene amplification for c-erbB-2, c-myc, epidermal growth factor receptor, int-2, and N-myc measured by quantitative PCR with a multiple competitor template. *Clin. Chem.*, **41**, 826–832.
44. Lyon,E., Millson,A., Lowery,M.C., Woods,R. and Wittwer,C.T. (2001) Quantification of HER2/neu gene amplification by competitive pcr using fluorescent melting curve analysis. *Clin. Chem.*, **47**, 844–851.
45. Millson,A., Suli,A., Hartung,L., Kunitake,S., Bennett,A., Nordberg,M.C., Hanna,W., Wittwer,C.T., Seth,A. and Lyon,E. (2003) Comparison of two quantitative polymerase chain reaction methods for detecting HER2/neu amplification. *J. Mol. Diagn.*, **5**, 184–190.
46. Dati,C., Antoniotti,S., Taverna,D., Perroteau,I. and De Bortoli,M. (1990) Inhibition of c-erbB-2 oncogene expression by estrogens in human breast cancer cells. *Oncogene*, **5**, 1001–1006.
47. Hynes,N.E., Gerber,H.A., Saurer,S. and Groner,B. (1989) Overexpression of the c-erbB-2 protein in human breast tumor cell lines. *J. Cell Biochem.*, **39**, 167–173.
48. Kallioniemi,O.P., Kallioniemi,A., Kurisu,W., Thor,A., Chen,L.C., Smith,H.S., Waldman,F.M., Pinkel,D. and Gray,J.W. (1992) ERBB2 amplification in breast cancer analyzed by fluorescence in situ hybridization. *Proc. Natl Acad. Sci. USA*, **89**, 5321–5325.
49. Pauletti,G., Godolphin,W., Press,M.F. and Slamon,D.J. (1996) Detection and quantitation of HER-2/neu gene amplification in human breast cancer archival material using fluorescence in situ hybridization. *Oncogene*, **13**, 63–72.